Published in final edited form as:
Sci Signal. ; 9(449): ra100. doi:10.1126/scisignal.aaf6625.

Pressure-induced oxidative activation of PKG enables vasoregulation by Ca^{2+} sparks and BK channels

Kaivan Khavandi[#1,2], **Rachael A. Baylie**[#1], **Sarah A. Sugden**[1], **Majid Ahmed**[1,3], **Viktoria Csato**[1,4], **Philip Eaton**[2], **David C. Hill-Eubanks**[3], **Adrian D. Bonev**[3], **Mark T. Nelson**[1,3], and **Adam S. Greenstein**[1,†]

[1]Institute of Cardiovascular Sciences, Faculty of Medical and Human Sciences, University of Manchester, Manchester Academic Health Sciences Center, Manchester, M13 9NT, UK

[2]King's College London, Cardiovascular Division, The British Heart Foundation Centre of Excellence, The Rayne Institute, Saint Thomas' Hospital, London, SE1 7EH, UK

[3]Department of Pharmacology, University of Vermont, Vermont, 05405-0068, USA

[4]Division of Clinical Physiology, Institute of Cardiology, Research Centre for Molecular Medicine, Faculty of Medicine, University of Debrecen, Debrecen 4012, Hungary

[#] These authors contributed equally to this work.

Abstract

Activation of Ca^{2+}-sensitive, large-conductance potassium (BK) channels in vascular smooth muscle cells (VSMCs) by local, ryanodine receptor-mediated Ca^{2+} signals (Ca^{2+} sparks) acts as a brake on pressure-induced (myogenic) vasoconstriction—a fundamental mechanism that regulates blood flow in small resistance arteries. Here, we report that physiological intraluminal pressure within resistance arteries activated cGMP-dependent protein kinase (PKG) in VSMCs through oxidant-induced formation of an intermolecular disulfide bond between cysteine residues. Oxidant-activated PKG was required to trigger Ca^{2+} sparks, BK channel activity, and vasodilation in response to pressure. VSMCs from arteries from mice expressing a form of PKG that could not be activated by oxidants showed reduced Ca^{2+} spark frequency, and arterial preparations from these mice had decreased pressure-induced activation of BK channels. Thus, the absence of oxidative activation of PKG disabled the BK channel-mediated negative feedback regulation of vasoconstriction. Our results support the concept of a negative feedback control mechanism that regulates arterial diameter through mechanosensitive production of oxidants to activate PKG and enhance Ca^{2+} sparks.

[†]Corresponding author: adam.greenstein@manchester.ac.uk.

Author contributions: KK designed experiments, performed pressure myography, genotyping, imaging protocols and analyzed data. RB designed experiments, performed pressure myography, imaging protocols, patch clamp electrophysiology and analyzed data. SS performed genotyping and western blot protocols. MA designed experiments, performed pressure myography and ROS imaging. VC designed experiments, performed pressure myography and calcium imaging. PE designed experiments, interpreted data and wrote the manuscript. DHE designed experiments and performed imaging protocols. AB designed ROS imaging, wrote new analysis software and analyzed results. MN designed the study, interpreted and analyzed data and wrote the manuscript. AG designed experiments, perfomed calcium imaging protocols, analyzed data and wrote the manuscript.

Competing interests: The authors declare that they have no competing interests.

Europe PMC Funders Author Manuscripts

Introduction

Resistance arteries react to increases in blood pressure through membrane potential depolarization, activation of voltage-dependent Ca^{2+} channels (VDCCs), and vasoconstriction, a process termed the myogenic response, which as its name implies is intrinsic to vascular smooth muscle cells (VSMCs). This pressure-induced constriction is buffered by concurrent activation of large-conductance, Ca^{2+}-sensitive potassium (BK) channels, which causes membrane potential hyperpolarization and deactivation of VDCCs, thereby decreasing Ca^{2+} influx and dampening constriction. Activation of BK channels in response to pressure is controlled by local, ryanodine receptor (RyR)-mediated Ca^{2+} signals (Ca^{2+} sparks) in the sarcoplasmic reticulum (SR) adjacent to the surface membrane1. The gain of this negative-feedback module determines the degree of vasoconstriction, and hence blood flow.

The increase in intracellular Ca^{2+} caused by pressure-induced membrane potential depolarization and activation of VDCCs has traditionally thought to set the gain of this system by controlling SR Ca^{2+} load and, hence, Ca^{2+} spark activity2,3. Stimulation of BK channel activity by the nitric oxide (NO)/soluble guanylate cyclase (sGC)/cGMP-dependent protein kinase (PKG) pathway, which is important in mediating the effects of endothelial-dependent vasodilators, is not thought to be involved in modulating the myogenic response of small resistance arteries during basal tone because there is no evidence for pressure-induced release of NO from the endothelium4–7. Under physiological conditions, PKG exists as a dimer and oxidants such H_2O_2 promote the formation of a disulfide bond between appositioned cysteine residues (Cys^{42}) within PKG dimers8. This disulfide bond within the PKG dimer results in physiological activation of the kinase independently of cGMP8. A PKG variant with a $Cys^{42}\rightarrow$Ser mutation (PKG[C42S] variant) is resistant to oxidant-induced activation9. In PKG[C42S] knock-in ($PKG[C42S]^{KI}$) mice, PKG[C42S] can still be activated by the traditional NO/sGC/cGMP pathway, and in response to stimulation of this pathway, resistance arteries from these mice show dilation to a similar extent as those from wild-type mice9. Intriguingly however, $PKG[C42S]^{KI}$ mice display a mildly hypertensive phenotype9.

Here, we showed that pressure-induced activation of BK channels was absent in $PKG[C42S]^{KI}$ mice, resulting in loss of the BK channel-mediated brake on pressure-induced constriction. We further found that pressure caused an increase in intracellular reactive oxygen species (ROS) that induced oxidative activation of PKG, an effect that was lost in $PKG[C42S]^{KI}$ mice. Collectively, our findings support a model in which pressure leads to NO/sGC/cGMP pathway-independent activation of PKG through oxidant-induced activation of PKG which in turn increases Ca^{2+} spark activity. The frequency of Ca^{2+} sparks within VSMCs is determined by this pressure-oxidant-PKG mechanism, which increases BK channel activity to regulate vascular physiology.

Results

Activation of BK channels by intraluminal pressure depends on oxidant-induced dimerization of PKG

To explore the basis for the increased blood pressure in PKG[C42S]^{KI} mice, we first assessed the constriction of resistance-sized (third-order branch) mesenteric arteries from these mice compared with those from wild-type mice. At a pressure that does not induce a myogenic response (20 mmHg), inhibition of BK channels with paxilline did not affect the diameter of resistance-sized mesenteric arteries from wild-type or PKG[C42S]^{KI} mice (Fig. 1, A, B)). Increasing intravascular pressure to physiological values (80 mmHg) constricted arteries from both wild-type and PKG[C42S]^{KI} mice (Fig. 1, C and D). Treatment with the BK channel inhibitor paxilline caused a marked, sustained constriction of arteries from wild-type mice (Fig. 1C), consistent with a vasodilatory influence of BK channels under myogenic conditions. Notably, inhibition of BK channels with paxilline had either no effect (Fig. 1D) or caused only a brief, transient constriction (fig. S1A) in pressurized (80 mmHg) arteries from PKG[C42S]^{KI} mice, demonstrating that BK channels play little or no role in modulating myogenic tone in the absence of oxidant-activatable PKG. Consistent with this finding, intraluminal pressure constricted the arteries from PKG[C43S]^{KI} mice to a considerably greater degree than those from wild-type mice (Fig. 1, C to E). Inhibition of BK channels eliminated this difference (Fig. 1, E to G), confirming that the greater constriction in arteries from PKG[C42S]^{KI} mice was attributable to the loss of BK channel-mediated negative feedback control over myogenic tone1. Collectively, these data suggest that oxidant-activated PKG was crucial for the activation of BK channels necessary to counteract pressure-induced constriction.

We have previously reported that inhibition of endothelial nitric oxide synthase (eNOS) with N^{ω}-nitro-*L*-arginine (L-NNA) does not affect myogenic tone in murine mesenteric arteries4, consistent with the absence of a role for the NO/sGC/cGMP pathway during pressure-induced constriction4–7. Similarly, inhibition of sGC with 1H-[1,2,4]oxadiazolo[4,3,-a]quinoxalin-1-one (ODQ) had no effect on the diameter of pressure (80 mmHg)-constricted mesenteric arteries from wild-type or PKG[C42S]^{KI} mice (fig. S1B). Notably, however, the synthetic oligopeptide DT-2, a direct inhibitor of PKG that does not distinguish between oxidant- and cGMP-activated PKG10,11, constricted pressurized (80 mmHg) mesenteric arteries from wild-type mice (fig. S1, B and C), but did not affect arteries from PKG[C42S]^{KI} mice (fig. S1, B and D). Since wild-type PKG and PKG[C42S] differ primarily in their ability to undergo oxidant activation, these results further support the central importance of NO/sGC/cGMP-independent activation of PKG in opposing the effects of pressure-induced constriction. Moreover, the effects of PKG inhibition with DT-2 and BK channel inhibition with paxilline were not additive (fig. S1E), and both inhibitors constricted pressurized (80 mmHg) wild-type arteries to a similar degree (fig. S1B, compare first and last sets of bars), indicating that PKG and the Ca^{2+} spark/BK channel module act in series. This finding suggests that oxidant-activated PKG largely acts through BK channels to regulate arterial tone.

Physiological pressure induces oxidant production

To confirm that physiological pressure activates PKG by inducing its covalent dimerization, we assessed PKG protein in pressurized arteries treated with the oxidant H_2O_2 by western blot analysis. Non-oxidized, monomeric wild-type PKG ran as a single band with a molecular weight of ~75 kD, whereas oxidant treatment induced formation of a band with an apparent molecular weight of ~150 kD (fig. S2A), reflecting the formation of covalently linked, dimerized PKG. As expected, PKG[C42S] ran at approximately the same position as wild-type PKG, but did not form a dimer in response to H_2O_2 treatment. At 20 mmHg, approximately 3% of PKG was dimerized in individual mesenteric arteries (fig. S2B). Increasing pressure to 80 mmHg modestly, but significantly increased the degree of oxidative dimerization of PKG to 7.4%. By comparison, the maximum dimerization of PKG that could be induced by a high concentration of H_2O_2 was ~16% (fig. S2A), indicating that physiological amounts of PKG dimerization are below the maximum.

To assess arterial production of oxidants in response to changes in intravascular pressure, we imaged arteries loaded with the ROS indicator dye CM-H_2DCFDA (Fig. 2A). Consistent with a previous report12, increasing intraluminal pressure from 20 to 80 mmHg increased oxidant production (Fig. 2B). The increase in oxidant-related fluorescence caused by pressurization from 20 to 80 mmHg was similar to that caused by application of 30 μM H_2O_2 to an artery pressurized to 20 mmHg (Fig. 2, A, B and C and fig. S3).

Oxidant-activated PKG increases Ca^{2+} spark activity rather than directly activating the BK channel

Our results suggest that intravascular pressure activates PKG through oxidant-induced disulfide bond formation, and further that oxidant-activated PKG decreases tone by activating BK channels. PKG can activate BK channels directly through phosphorylation13,14 or indirectly by stimulating Ca^{2+} sparks15,16. We first tested the possible effects of PKG[C42S]^{KI} on BK channel currents, measured in the conventional whole-cell mode with ryanodine present to silence ryanodine receptor-mediated Ca^{2+} sparks. Whole-cell BK channel currents were similar in VSMCs isolated from arteries of wild-type and PKG[C42S]^{KI} mice (Fig. 3, A to C), indicating that a reduction in BK channel current density was not responsible for loss of the BK channel-mediated brake on pressure-induced tone. Application of H_2O_2 (100 μM) also did not affect BK channel currents in isolated cells, as measured in the cytoplasm-intact, perforated-patch configuration in the presence of ryanodine (fig. S4, A to C). These results indicate that oxidant activated PKG does not directly activate BK channels in mesenteric VSMCs.

Under physiological conditions, the primary activators of BK channels are Ca^{2+} sparks1. A Ca^{2+} spark activates approximately 30 nearby BK channels to induce a transient K^+ current, referred to as a spontaneous transient outward current (STOC) 1,17. Using the perforated-patch configuration, we measured whole-cell currents in isolated VSMCs from wild-type and PKG[C42S]^{KI} arteries at a physiological membrane potential (-40 mV) as well as at more depolarized membrane potentials (-20 and 0 mV), given the voltage dependence of both Ca^{2+} sparks and BK channels. Consistent with previous studies, membrane depolarization increased STOC amplitude and frequency in myocytes from both wild-type

and PKG[C42S]^{KI} arteries (Fig. 3, D to F). STOCs were readily detected in wild-type cells voltage-clamped at -40 mV, but not in PKG[C42S]^{KI} cells held at the same membrane potential. Depolarization of PKG[C42S]^{KI} cells to -20 mV induced detectable STOCs, but their frequency and amplitude were significantly lower in these cells than in depolarized wild-type cells. These results suggested that oxidant activated PKG was active in isolated myocytes, and that membrane potential depolarization to -20 mV can overcome the lack of oxidizable PKG in PKG[C42S]^{KI} VSMCs. The decrease in STOC activity at -40 mV, combined with the lack of a direct effect on BK channel current density, supports the concept that Ca^{2+} spark activity was decreased in arteries from PKG[C42S]^{KI} mice.

We explored this hypothesis by imaging Ca^{2+} sparks in smooth muscle cells within intact mesenteric arteries pressurized to 20 or 80 mmHg using high-speed, spinning-disc confocal microscopy (Fig. 4 A and B). At 20 mmHg, arteries did not develop tone, and spark frequency was relatively low in both wild-type and PKG[C42S]^{KI} arteries. Increasing pressure to 80 mmHg increased Ca^{2+} spark frequency by ~7-fold in arteries from wild-type mice, but had no effect in arteries from PKG[C42S]^{KI} mice, supporting the idea that pressure acts through increased oxidant-induced activation of PKG to stimulate Ca^{2+} sparks. Similarly, application of H_2O_2 (30 μM) to wild-type arteries at 20 mmHg increased Ca^{2+} spark frequency to amounts comparable to those in untreated wild-type arteries pressurized to 80 mmHg, but had no effect on arteries from PKG[C42S]^{KI} mice (Fig. 4C). The temporal characteristics (rise time, duration, and decay) and increase in fractional fluorescence of individual spark events were unchanged between PKG[C42S]^{KI} and wild-type arteries (Fig. 4, D to F). Moreover, incubation with DT-2, which inhibits both cGMP- and oxidant-activated PKG, significantly reduced Ca^{2+} spark frequency in pressurized (80 mmHg) wild-type mesenteric arteries (fig. S5), consistent with diameter studies. By contrast, Rp-8-Br-PET-cGMPS, a selective inhibitor of cGMP-mediated PKG activation, had no effect on Ca^{2+} sparks in these pressurized WT arteries (fig. S5). These results are consistent with the concept that an increase in intravascular pressure increases Ca^{2+} sparks through oxidant-induced activation of PKG (fig. S7).

To investigate whether the difference in Ca^{2+} spark frequency between the wild-type and PKG[C42S]^{KI} arteries could be accounted for by differences in the Ca^{2+} content of the sarcoplasmic reticulum, we measured caffeine-induced Ca^{2+} transient amplitudes in intact arteries (fig. S6). However, there were no differences in the caffeine-induced Ca^{2+} transient amplitudes between wild-type and PKG[C42S]^{KI} arteries.

Discussion

Here, we report the discovery of an essential vasoregulatory negative-feedback element enabled by pressure-induced oxidants. Oxidants generated in response to intraluminal pressure activated PKG through formation of a disulfide bond between appositioned cysteine residues within the existing dimeric structure of the kinase. The resulting increase in PKG activity enhanced Ca^{2+} spark activity and sufficiently increased BK channel activity to exert an opposing influence on myogenic vasoconstriction. Because PKG[C42S] cannot be activated by oxidants, pressure failed to activate PKG in small mesenteric arteries from PKG[C42S]^{KI} mice. As a consequence, the BK-dependent vasodilation that moderates

pressure-induced constriction was absent in these arteries. Notably, direct application of H_2O_2 (30 μM) increased Ca^{2+} spark frequency in VSMCs from wild-type mice, but did not increase BK channel currents in these same cells treated with ryanodine to block Ca^{2+} sparks, further supporting the conclusion that oxidant-activated PKG increases BK channel-mediated vasodilation of arteries through an increase in Ca^{2+} spark frequency rather than a direct effect on the BK channel.

The importance of mechanical stimulus for physiological oxidant production in cardiovascular systems is increasingly appreciated. Physiological amounts of intraluminal pressure within resistance arteries from both skeletal12 and renal circulations18 generates superoxide through activation of nicotinamide adenine dinucleotide phosphate (NADPH) oxidase 2 (Nox2). Superoxide dismutase converts superoxide to H_2O_2 and both oxidant species are thought to regulate the vascular tone12,18. Similarly, in cardiac muscle cells, physiological stretch also generates ROS and, consistent with our findings in this study, the stretch-driven oxidant production rapidly increases Ca^{2+} spark activity19. In cardiomyocytes the stretch activation of Nox2 depends on an intact microtubular network19. However, the precise mechanisms by which mechanical stimuli activate Nox2 in myocytes are unclear. One potential candidate is the Angiotensin II receptor. This receptor has been reported to play a dual role in VSMCs, acting as both a pressure sensor to cause myogenic tone20, and as an activator of Nox, to increase ROS21. Indeed, angiotensin II type 1 receptors act as mechanosensors to engage beta-arrestin signaling22. These observations suggest a mechanism in which angiotensin II receptors20 or other GPCRs23 act to transduce intraluminal pressure into an increase in ROS while also causing membrane potential depolarization and vasoconstriction (fig. S7).

Left unanswered is the important question of the identity of the downstream phosphorylation target of oxidant-dimerized PKG within VSMCs. Two potential targets are the ryanodine receptor or the sarcoplasmic reticulum-ATPase (SERCA)/phospholamban complex. Phospholamban regulates sarcoplasmic reticulum Ca^{2+} load—and thus Ca^{2+} spark frequency—by inhibiting the activity of the sarcoplasmic reticulum-ATPase (SERCA)24. When phosphorylated, phospholamban inhibitory activity is relieved and furthermore, loss of phospholamban can increase sarcoplasmic reticulum Ca^{2+} load and Ca^{2+} spark frequency25. The relationship between sarcoplasmic reticulum Ca^{2+} load and spark frequency is non-linear, such that a potentially small increase sarcoplasmic reticulum Ca^{2+} could cause a substantial increase in spark frequency in smooth muscle26. An increase in Ca^{2+} spark frequency, such as from RyR activity, would tend to lower sarcoplasmic reticulum Ca^{2+} load, with the steady state sarcoplasmic reticulum Ca^{2+} content being determined by a balance between uptake (SERCA activity) and leak (RyR activity). The similar amplitudes of caffeine induced Ca^{2+} transients between wild-type and PKG[C42S]^{KI} arteries suggests that SR Ca^{2+} load does not differ between the two genotype and thus initially argues against phospholamban as the target for oxidized PKG. Conversely, phosphorylation of the ryanodine receptor directly by oxidized PKG might decrease sarcoplasmic reticulum Ca^{2+} load through increased leak. Indeed, Ca^{2+}-calmodulin Kinase (CaMK) and possibly Protein Kinase A (PKA) increase RyR Ca^{2+} sensitivity and thus open probability through phosphorylation of serine residues within the ryanodine receptor27,28. However, it is important to note that even if PKG did target the ryanodine receptor itself, it is not known

whether this would affect vascular Ca^{2+} spark frequency. Another caveat is the limitation in accuracy of the approach whereby sarcoplasmic reticulum Ca^{2+} load is estimated using caffeine induced transients from whole artery preparations. Given the importance of accurate determination sarcoplasmic reticulum of SR Ca^{2+} load in elucidating the downstream target of oxidized PKG, additional experiments are indicated, most likely involving single cell preparations. A single cell approach, possibly combining simultaneous patch clamp and Ca^{2+} spark imaging, would also be useful in identifying the target of oxidized PKG.

The frequency of transient BK currents (STOCs) that are activated by sparks was reduced in isolated myocytes from arteries of PKG[C42S]^{KI} mice, in accord with reduction of Ca^{2+} sparks measured in myocytes in intact pressurized arteries. However, the amplitudes of Ca^{2+} sparks were not changed in arteries from PKG[C42S]^{KI} mice, but the amplitudes of the STOCs were reduced. This apparent discrepancy could have various explanations aside from the use of enzymatically isolated cells at room temperature (patch clamp) by one measurement and the use of intact arteries at 37°C (imaging) for the other measurement. The Ca^{2+} spark amplitude is the increase in fractional fluorescence, and to translate this to Ca^{2+} concentration, the baseline Ca^{2+} concentration must be known. STOC amplitude reflects the change of open probability of a cluster of BK channels, which depends on the local increase in intracellular Ca^{2+} concentration during a spark, baseline open probability of the BK channel, and the number of BK channels engaged17. Thus, it is difficult to reach a meaningful conclusion from a simple comparison of spark and STOC amplitudes.

Irrespective of the downstream target of oxidized PKG, an important implication of our model is that the pressure-induced increase in Ca^{2+} spark activity reflects the operation of a binary mechanism that requires both a PKG-mediated increase in the Ca^{2+} spark activity and a concurrent increase in intracellular Ca^{2+} concentration caused by membrane potential depolarization-dependent activation of VDCCs2,3,15,16. The original conceptualization of Ca^{2+} spark-BK channel negative feedback control of arterial diameter posited that the increase in intracellular Ca^{2+} concentration in response to pressure-induced depolarization is sufficient to engage the Ca^{2+} spark-BK channel pathway and affect membrane potential1. Indeed, membrane depolarization of cerebral arteries to non-physiological membrane potentials (-20 mV) with high K^+ in unpressurized arteries3 or by voltage-clamp of isolated cerebral myocytes does increase Ca^{2+} spark and STOC frequency29. However, physiological intravascular pressure (80 mm Hg) causes a much less robust membrane depolarization of cerebral arteries (to about -45 mV), as well as a smaller rise in intracellular Ca^{2+} concentration30 (to about 200 nM). Although the pressure-induced increase in intracellular Ca^{2+} concentration is sufficient to cause pronounced vasoconstriction due to Ca^{2+}-calmodulin activation of myosin light chain kinase, SERCA activity in this setting would be predicted to be very low owing to low intracellular Ca^{2+} concentration and ongoing suppression by phospholamban, which would limit spark activity by inhibiting sarcoplasmic reticulum Ca uptake31. However, at 80 mmHg intraluminal pressure, Ca^{2+} spark frequency is increased, even with modest intracellular Ca^{2+} concentration. Our results can potentially resolve this dilemma because they demonstrated that through oxidation, intraluminal pressure also activated PKG, which we suspect then either indirectly or directly sensitized the ryanodine receptor to Ca^{2+} or phosphorylated phospholamban, thus disinhibiting SERCA (fig. S7). Either of these activation mechanisms could potentially boost Ca^{2+} spark

generation by the sarcoplasmic reticulum, either through increasing Ca^{2+} load (disinhibition of SERCA) or directly increasing the open probability of ryanodine receptors26. We propose that, in PKG[C42S]^{KI} mesenteric arteries, this capacity to engage the sarcoplasmic reticulum in response to pressure through oxidant activation of PKG is lost, thus explaining the observed lower Ca^{2+} spark frequency. An important caveat is that there is notable variation in the membrane potential of pressurized resistance arteries from different microcirculatory beds (for example, -35mV for skeletal muscle arteries 32,33 compared to -45mV for cerebral arteries34) so it will be important to examine this mechanism in arteries from different anatomical sites.

From a broader perspective, regulation of contractility through coupling of Ca^{2+} sparks to BK channels is a highly conserved characteristic of smooth muscle, not only in the vasculature but also in a various types of non-vascular smooth muscle35–37. Indeed, disruption of this pathway is a feature of several diseases, including diabetes38, hypertension39 and obesity40. Thus, understanding the mode of communication that links smooth muscle stretch and pressure to ion channel function through oxidant generation would be applicable for different pathophysiological situations.

In summary, we showed that oxidative activation of PKG was crucial for Ca^{2+} spark-mediated vasoregulation in pressure-constricted mesenteric arteries, providing an important reformulation of the classic model of Ca^{2+} sparks-BK channel feedback regulation of vasoconstriction. According to this refined paradigm, intraluminal pressure within arteries generated oxidants that activated PKG by causing disulfide bond formation between appositioned cysteine residues. Thus activated, PKG increased Ca^{2+} spark frequency to the amount necessary to engage BK channels and oppose the inherent myogenic constriction of the artery. Our observation places PKG at the center of a previously unsuspected intraluminal pressure-oxidant/PKG/Ca^{2+} spark/BK channel vasodilatory pathway that is critical to normal small artery vasoregulation and blood pressure control.

Materials and Methods

Animal Studies

Procedures were performed in accordance with the UK Home Office Guidance on the Operation of the Animals (Scientific Procedures) Act 1986 in United Kingdom and were approved by an institutional review committee. Animal procedures in this study performed in Vermont are in accord with institutional guidelines and were approved by the Institutional Animal Care and Use Committee of the University of Vermont. Mice constitutively expressing PKGIα [C42S] (referred to in the manuscript as PKG[C42S]^{KI}) were generated on a pure C57BL/6j background by Taconic Artemis (Koln, Germany) as described previously by the Eaton group9. Colonies in Manchester were replenished annually by breeding PKG[C42S]^{KI} mice with commercially obtained C57Bl/6j mice to generate heterozygous mice. From these heterozygotes, either wild-type or PKG[C42S]^{KI} colonies were generated by breeding and genotyping. Age-matched (12-week-old) male wild-type and PKG[Cys42Ser]^{KI} mice were used in all studies. Mice had ad libitum access to standard chow and water and were kept in specific pathogen-free conditions under a 12-hour day/night cycle. Mice were euthanized using a Schedule 1 procedure (cervical dislocation). The

mesenteric bed was removed and kept in an ice-cold HEPES-buffered physiological saline solution (HEPES-PSS) with the following composition: 134 mM NaCl, 6 mM KCl, 1 mM $MgCl_2$, 2 mM $CaCl_2$, 7 mM glucose and 10 mM HEPES, with pH adjusted to 7.4 with 1 M NaOH.

Genotyping of mice

Mice were genotyped using the REDExtract-N-Amp Tissue PCR kit from Sigma-Aldrich (St Louis, MO, USA), as described by the manufacturer. Briefly, genomic DNA was extracted by mixing ear snip tissue (2–3 mm) with freshly made Extraction Solution and Tissue Preparation Solution (4:1) and incubating at room temperature for 10 minutes. Tissue was then incubated at 95°C for 3 minutes and mixed with a third solution to neutralize inhibitory substances prior to PCR. The extract was mixed with PCR ReadyMix; the $PKG[C42S]^{KI}$-specific primers, 5'-cag ttt agg gac aga gtt gg-3' (forward) and 5'-aac ctg ctt cat gcg caa gg-3 (reverse) were used in the reaction at a final concentration of 0.4 μM.

Chemicals

All chemicals were from Sigma (Welwyn, UK), apart from the PKG inhibitor DT-2, which was obtained from Biolog Life Science Institute (Bremen, Germany).

Immunoblotting

Non-reducing SDS-polyacrylamide gel electrophoresis was carried out using a Bio-Rad system (Hercules, CA, USA). After electrophoresis, samples were transferred to polyvinylidene difluoride (PVDF) membranes using a Bio-Rad semidry blotter. Membranes were blocked with 10% non-fat dry milk in phosphate-buffered saline (PBS) containing 0.1% Tween-20 (PBS-T) for 1 hour at room temperature and then immunostained for PKG1α (ADI-KAP-K005-F PKG; Enzo Life Sciences, Exeter, UK) as previously documented8,9. Monomeric (~75 kDa) and dimeric (~150 kDa) forms of PKG were quantified using ImageJ software.

Pressure myography

Third-order branches of mesenteric arteries (~130–150 μm internal diameter) were dissected free of surrounding tissue and mounted on borosilicate glass pipettes in an arteriograph chamber (Living Systems Instrumentation, St. Albans, VT, USA). The proximal glass pipette was attached to a servo-controlled pressure-regulating device (Living Systems Instrumentation), and the distal pipette was blocked. After checking for leaks, arteries were pressurized to 80 mmHg for approximately 45 minutes in physiological saline solution (PSS) with the following composition: 119 mM NaCl, 4.7 mM KCl, 1.2 mM KH_2PO_4, 1.2 mM $MgCl_2$, 2 mM $CaCl_2$, 7 mM glucose, 24 mM NaHCO3, and 2.3 mM EDTA. PSS was warmed to 37°C and continuously gassed with biological gas (95% air and 5% CO_2). Arteries exhibiting a leak were discarded, and pharmacological protocols were only performed on arteries that exhibited pressure-induced myogenic tone. Internal diameter was detected using a CCD camera and Living Systems edge-detection software. Pressurized arteries were exposed to circulating PSS and allowed to develop myogenic tone, defined as the difference between the vessel diameter in Ca^{2+}-containing and Ca^{2+}-free solutions,

expressed as a percentage of the diameter in Ca^{2+}-free conditions. Dilation or constriction to drugs was expressed as a change in the percentage of overall active tone.

Imaging of oxidants in pressurized arteries

Third-order branches of mesenteric arteries were isolated from male C57BL/6 mice (8–12 weeks old), cleaned of surrounding connective tissue, and mounted onto a glass cannula in an arteriograph chamber as described above. Arteries were pressurized to 20 mmHg and superfused with PSS at 37°C for 60 minutes. Following this equilibration period, arteries were loaded with 10 μM 5-(and-6)-chloromethyl-2′,7′-dichlorodihydrofluorescein diacetate (CM-H_2DCFDA), a sensor of ROS (hydroxyl radicals, superoxide, H_2O_2 – although the latter indirectly41), at 37°C for 45 minutes. CM-H_2DCFDA is a cell-permeant non-fluorescent fluorescein-based indicator that contains an additional chloromethyl group that aids cellular retention. Upon entry of CM-H_2DCFDA into cells, the acetate group is removed by intracellular esterases and oxidation leads to a fluorescent adduct. Because DCF-based dyes both photo-oxidize and auto-oxidize in the absence of external oxidants41,42, arteries were loaded in the dark, and the remainder of the experiment from this point was conducted under dark conditions. After loading the oxidant sensor, the arteries were washed with PSS for 5 minutes. Fluorescent images of arteries focusing on the vascular smooth muscle cell layer were then recorded at a rate of 0.1 Hz on an epifluorescence microscope (Andor Technology, Belfast, UK) using an excitation wavelength of 480 nm and an emission wavelength of 535 nm. All arteries remained pressurized at 20 mmHg for the first 4 minutes of the recording. Arteries were then subjected to one of three protocols: (i) intraluminal pressure was maintained at 20 mmHg, to account for auto-oxidation; (ii) intraluminal pressure was maintained at 20 mmHg, but arteries were treated with 30 μM H_2O_2, added to the PSS superfusate (‘positive control group’); and (iii) intraluminal pressure was increased to 80 mmHg for 4 minutes and then returned to 20 mmHg (no H_2O_2 added to the superfusate). Custom-written software (Sparkan) designed by Adrian Bonev was used for analyses. A fluorescence trace was recorded within a large region of interest (range 23–74 μm^2) placed over the central region of arteries loaded with 10 μM CM-H_2DCFDA at a point where focus on the vascular smooth muscle cell layer was uniform. Increases in CM-H_2DCFDA fluorescence were quantified relative to the first image and presented as a ratio (F/F_0). Because the position of the artery sometimes moved from frame to frame, a tracking algorithm was used to ensure that fluorescence was collected from the same region of interest (ROI). Pressurization to 80 mmHg increased the diameters of arteries and caused a shift in the position of the vessel that was sufficiently large to prevent the software from being able to efficiently track a given ROI. Therefore, in this pressure group, pressure was restored to 20 mmHg after 4 minutes and the artery was allowed to return to its original position, a protocol similar to that described previously12, allowing our tracking algorithm to locate the original ROI. The fluorescence of these arteries (group 3) was determined 1 minute after returning to 20 mmHg (following 80 mmHg) and compared to the equivalent time points in the oxidant control (30 μM H_2O_2) and pressure control (20 mmHg) groups.

High-speed spinning-disc confocal microscopy

Mesenteric arteries were placed in HEPES-PSS containing 10 μM Fluo-4-AM and 0.05% pluronic acid for 1 hour at room temperature, followed by a 30-minute wash in HEPES-PSS. Arteries were subsequently mounted on glass pipettes in an arteriograph chamber (as described above), pressurized to either 20 or 80 mmHg in circulating PSS (composition as above), and gassed with 95% air and 5% CO_2. Ca^{2+} sparks were imaged with an Andor confocal system (Andor Technology) consisting of a Nikon upright microscope with a 60x, water-dipping objective (NA 1.0) and an electron-multiplying CCD camera. Images were acquired with Andor Revolution acquisition software at 55 frames/s. Bound Ca^{2+} was detected by exciting at 488 nm and collecting emitted fluorescence using a 527.5/49 bandpass filter. Video files of Ca^{2+} sparks of arteries were obtained at a single time point (such that there were no repeated images before and after incubation with drugs). Ca^{2+} sparks were identified using custom-written software (Sparkan; Dr A. Bonev) that detects temporally delineated increases in fractional fluorescence (F) greater than 1.26 above baseline fluorescence amounts (F_o) in a defined, 1.1 × 1.1 μm area of interest (5 × 5 pixels); Ca^{2+} increases were expressed as F/F_o. Two areas from each artery were analyzed for each experiment, and the average of these was used for analysis (such that the average of two areas from one artery constituted a single biological replicate).

Imaging of caffeine induced calcium transients in intact pressurized arteries

Mesenteric arteries were loaded with Fluo-4-AM and subsequently pressurized to 80mmHg in an arteriography chamber as described above. To prevent caffeine induced movement and thus loss of focus, the arteries were also co-incubated with 1μM Wortmannin (which does not affect caffeine transients in myocytes43). Caffeine induced (10mM) calcium transients were imaged using the Andor confocal system (as above) with images acquired at 1 Hz with a 50ms exposure through a 20sx water dipping objective (NA 1.0). Arteries were exposed to caffeine for 2 minutes during a 9-10 minute recording period. Changes in fractional fluorescence (F/Fo) in response to caffeine was analysed using custom written software (Sparkan: Adrian Bonev). The change in F/Fo was calculated for the entire field of view and obtained by dividing the fluorescence of the region of interest by the average fluorescence of 10 images without activity from the same region of interest. The area under the curve (AUC) for each of the caffeine transients was calculated using a trapezoidal numerical integration ([F – Fo]/Fo over time).

Single-cell isolation

Mesenteric arteries were dissected free from surrounding tissue and cut into smaller segments before being placed in a cell isolation solution containing 10 mM HEPES (pH 7.4), 55 mM NaCl, 80 mM Na-glutamate, 5.6 mM KCl, 2 mM $MgCl_2$, and 10 mM glucose. Artery segments were incubated in 2.0 mg/ml papain (Worthington Biochemical Corp., Lakewood NJ, USA) and 1.0 mg/ml dithioerythritol (Sigma, Welwyn, UK) for 20 minutes at 37°C and then in 1.0 mg/ml Type F collagenase (Sigma, Welwyn, UK) for 7 minutes at 37°C. Digested segments were washed with cell isolation solution, triturated to liberate single smooth muscle cells, and then stored on ice until used.

Patch-clamp recordings: Spontaneous transient outward currents

Isolated smooth muscle cells were placed into a recording chamber and allowed to adhere to glass coverslips for 20 minutes at room temperature. Whole-cell currents were recorded with an AxoPatch 200B amplifier (Molecular Devices, Sunnyvale, CA, USA) equipped with an Axon CV 203BU headstage (Molecular Devices). Recording electrodes (~4–5 MΩ) were used to obtain a gigaohm seal. For perforated patch, whole-cell measurements, the bath solution contained 10 mM HEPES (pH 7.4), 134 mM NaCl, 6 mM KCl, 1 mM $MgCl_2$, 2 mM $CaCl_2$, and 10 mM glucose. The pipette solution contained 10 mM HEPES, 85 mM K-aspartate, 1 mM $MgCl_2$, 30 mM KCl, 10 mM NaCl and 5 μM EGTA, with pH adjusted to 7.2 with KOH. Nystatin (200 μg/ml) was included in the pipette solution to perforate the cell membrane. STOCs were recorded using Clampex software, version 10.4 (Molecular Devices), at -40, -20 and 0 mV. Membrane currents were filtered at 1 kHz and sampled at 2 kHz. STOC amplitude and frequency were calculated using a threshold analysis in Clampfit version 10.4 (Molecular Devices). The threshold was set to three times the single-channel amplitude.

Patch-clamp recordings: Voltage step current

For conventional whole-cell experiments, the pipette solution contained 10 mM HEPES, 110 mM K-aspartate, 1 mM $MgCl_2$, 30 mM KCl, 10 mM NaCl, 5 mM EGTA and 2.5 mM $CaCl_2$, with pH adjusted to 7.2 with KOH. Free Ca^{2+} was 200 nM, calculated using the online Ca-Mg-ATP-EGTA calculator V1.0 using constants from NIST database #46 V8 (http://maxchelator.stanford.edu/CaMgATPEGTA-NIST.htm). Outward currents were measured during 250-ms voltage steps from -40 mV to +50 mV in 10-mV increments, from a holding potential of -50 mV, in the presence or absence of the selective BK channel inhibitor, paxilline (1 μM). BK current amplitude was estimated from difference currents (±paxilline) calculated using Clampex 10.4. All recordings were performed at room temperature (~22°C). Corrections for liquid junction potentials were applied using the amplifier prior to recordings. For perforated-patch protocols with voltage-stepped current measurements, the pipette and bath solutions were the same as outlined above for the measurement of STOCs with nifedipine and ryanodine in the bath solution.

Statistics

Group differences were analyzed using analysis of variance (ANOVA) and Student's t-test (independent samples) or non-parametric tests, as appropriate. All continuous data were assessed for normality of distribution using the Shapiro Wilk test. A 95% confidence level ($P < 0.05$) was taken as significant. All statistics were performed using SPSS v.16.

Supplementary Materials

Refer to Web version on PubMed Central for supplementary material.

Acknowledgments

We also thank Dr. George Wellman for making equipment available and helping us with its use.

Europe PMC Funders Author Manuscripts

Funding: This research was funded by grants to AG (British Heart Foundation FS/14/26/30767, IG/13/4/30317, FS/12/81/29882, PG/15/109/31931), MTN (NIH; 1P01HL095488, R37DK053832, and R01HL098243, 1R01HL131181, R01HL121706; Totman Medical Research Trust, Horizon 2020 and Fondation Leducq) and PE (British Heart Foundation FS/11/45/28859, RG/12/12/29872, Medical Research Council, Fondation Leducq, European Research Council and Department of Health via the National Institute for Health Research Comprehensive Biomedical Research Centre award to Guy's and Saint Thomas' National Health Service Foundation Trust).

References and Notes

1. Nelson MT, Cheng H, Rubart M, et al. Relaxation of arterial smooth muscle by calcium sparks. Science. 1995 Oct 27; 270(5236):633–637. [PubMed: 7570021]
2. Jaggar JH. Intravascular pressure regulates local and global Ca(2+) signaling in cerebral artery smooth muscle cells. Am J Physiol Cell Physiol. 2001 Aug; 281(2):C439–448. [PubMed: 11443043]
3. Jaggar JH, Stevenson AS, Nelson MT. Voltage dependence of Ca2+ sparks in intact cerebral arteries. The American journal of physiology. 1998 Jun; 274(6 Pt 1):C1755–1761. [PubMed: 9611142]
4. Sonkusare SK, Bonev AD, Ledoux J, et al. Elementary Ca2+ signals through endothelial TRPV4 channels regulate vascular function. Science. 2012 May 4; 336(6081):597–601. [PubMed: 22556255]
5. Murphy TV, Kotecha N, Hill MA. Endothelium-independent constriction of isolated, pressurized arterioles by Nomega-nitro-L-arginine methyl ester (L-NAME). Br J Pharmacol. 2007 Jul; 151(5): 602–609. [PubMed: 17471179]
6. Schubert R, Lehmann G, Serebryakov VN, Mewes H, Hopp HH. cAMP-dependent protein kinase is in an active state in rat small arteries possessing a myogenic tone. The American journal of physiology. 1999 Sep; 277(3 Pt 2):H1145–1155. [PubMed: 10484437]
7. Reimann K, Krishnamoorthy G, Wangemann P. NOS inhibition enhances myogenic tone by increasing rho-kinase mediated Ca2+ sensitivity in the male but not the female gerbil spiral modiolar artery. PLoS One. 2013; 8(1):e53655. [PubMed: 23301097]
8. Burgoyne JR, Madhani M, Cuello F, et al. Cysteine redox sensor in PKGIa enables oxidant-induced activation. Science. 2007 Sep 7; 317(5843):1393–1397. [PubMed: 17717153]
9. Prysyazhna O, Rudyk O, Eaton P. Single atom substitution in mouse protein kinase G eliminates oxidant sensing to cause hypertension. Nat Med. 2012 Feb; 18(2):286–290. [PubMed: 22245782]
10. Dostmann WR, Taylor MS, Nickl CK, Brayden JE, Frank R, Tegge WJ. Highly specific, membrane-permeant peptide blockers of cGMP-dependent protein kinase Ialpha inhibit NO-induced cerebral dilation. Proc Natl Acad Sci U S A. 2000 Dec 19; 97(26):14772–14777. [PubMed: 11121077]
11. Nickl CK, Raidas SK, Zhao H, et al. (D)-Amino acid analogues of DT-2 as highly selective and superior inhibitors of cGMP-dependent protein kinase Ialpha. Biochim Biophys Acta. 2010 Mar; 1804(3):524–532. [PubMed: 20018259]
12. Nowicki PT, Flavahan S, Hassanain H, et al. Redox signaling of the arteriolar myogenic response. Circulation research. 2001 Jul 20; 89(2):114–116. [PubMed: 11463716]
13. Fukao M, Mason HS, Britton FC, Kenyon JL, Horowitz B, Keef KD. Cyclic GMP- dependent protein kinase activates cloned BKCa channels expressed in mammalian cells by direct phosphorylation at serine 1072. The Journal of biological chemistry. 1999 Apr 16; 274(16):10927–10935. [PubMed: 10196172]
14. Robertson BE, Schubert R, Hescheler J, Nelson MT. cGMP-dependent protein kinase activates Ca-activated K channels in cerebral artery smooth muscle cells. Am J Physiol. 1993 Jul; 265(1 Pt 1):C299–303. [PubMed: 8338137]
15. Jaggar JH, Wellman GC, Heppner TJ, et al. Ca2+ channels, ryanodine receptors and Ca(2+)-activated K+ channels: a functional unit for regulating arterial tone. Acta physiologica Scandinavica. 1998 Dec; 164(4):577–587. [PubMed: 9887980]
16. Porter VA, Bonev AD, Knot HJ, et al. Frequency modulation of Ca2+ sparks is involved in regulation of arterial diameter by cyclic nucleotides. The American journal of physiology. 1998 May; 274(5 Pt 1):C1346–1355. [PubMed: 9612222]

17. Perez GJ, Bonev AD, Nelson MT. Micromolar Ca(2+) from sparks activates Ca(2+)- sensitive K(+) channels in rat cerebral artery smooth muscle. Am J Physiol Cell Physiol. 2001 Dec; 281(6):C1769–1775. [PubMed: 11698234]
18. Ren Y, D'Ambrosio MA, Liu R, Pagano PJ, Garvin JL, Carretero OA. Enhanced myogenic response in the afferent arteriole of spontaneously hypertensive rats. Am J Physiol Heart Circ Physiol. 2010 Jun; 298(6):H1769–1775. [PubMed: 20363886]
19. Prosser BL, Ward CW, Lederer WJ. X-ROS signaling: rapid mechano-chemo transduction in heart. Science. 2011 Sep 9; 333(6048):1440–1445. [PubMed: 21903813]
20. Schleifenbaum J, Kassmann M, Szijarto IA, et al. Stretch-activation of angiotensin II type 1a receptors contributes to the myogenic response of mouse mesenteric and renal arteries. Circulation research. 2014 Jul 7; 115(2):263–272. [PubMed: 24838176]
21. Lassegue B, Sorescu D, Szocs K, et al. Novel gp91 (phox) homologues in vascular smooth muscle cells : nox1 mediates angiotensin II-induced superoxide formation and redox-sensitive signaling pathways. Circulation research. 2001 May 11; 88(9):888–894. [PubMed: 11348997]
22. Tang W, Strachan RT, Lefkowitz RJ, Rockman HA. Allosteric modulation of beta-arrestin-biased angiotensin II type 1 receptor signaling by membrane stretch. The Journal of biological chemistry. 2014 Oct 10; 289(41):28271–28283. [PubMed: 25170081]
23. Li Y, Baylie RL, Tavares MJ, Brayden JE. TRPM4 channels couple purinergic receptor mechanoactivation and myogenic tone development in cerebral parenchymal arterioles. J Cereb Blood Flow Metab. 2014 Oct; 34(10):1706–1714. [PubMed: 25099756]
24. Wellman GC, Nelson MT. Signaling between SR and plasmalemma in smooth muscle: sparks and the activation of Ca2+-sensitive ion channels. Cell calcium. 2003 Sep; 34(3):211–229. [PubMed: 12887969]
25. Wellman GC, Santana LF, Bonev AD, Nelson MT. Role of phospholamban in the modulation of arterial Ca(2+) sparks and Ca(2+)-activated K(+) channels by cAMP. Am J Physiol Cell Physiol. 2001 Sep; 281(3):C1029–1037. [PubMed: 11502581]
26. ZhuGe R, Tuft RA, Fogarty KE, Bellve K, Fay FS, Walsh JV Jr. The influence of sarcoplasmic reticulum Ca2+ concentration on Ca2+ sparks and spontaneous transient outward currents in single smooth muscle cells. The Journal of general physiology. 1999 Feb; 113(2):215–228. [PubMed: 9925820]
27. Camors E, Valdivia HH. CaMKII regulation of cardiac ryanodine receptors and inositol triphosphate receptors. Frontiers in pharmacology. 2014; 5:101. [PubMed: 24847270]
28. Valdivia HH. Ryanodine receptor phosphorylation and heart failure: phasing out S2808 and “criminalizing” S2814. Circulation research. 2012 May 25; 110(11):1398–1402. [PubMed: 22628571]
29. Jaggar JH, Porter VA, Lederer WJ, Nelson MT. Calcium sparks in smooth muscle. Am J Physiol Cell Physiol. 2000 Feb; 278(2):C235–256. [PubMed: 10666018]
30. Knot HJ, Nelson MT. Regulation of arterial diameter and wall [Ca2+] in cerebral arteries of rat by membrane potential and intravascular pressure. The Journal of physiology. 1998 Apr 1; 508(Pt 1): 199–209. [PubMed: 9490839]
31. Cantilina T, Sagara Y, Inesi G, Jones LR. Comparative studies of cardiac and skeletal sarcoplasmic reticulum ATPases. Effect of a phospholamban antibody on enzyme activation by Ca2+ The Journal of biological chemistry. 1993 Aug 15; 268(23):17018–17025. [PubMed: 8349590]
32. Emerson GG, Segal SS. Electrical coupling between endothelial cells and smooth muscle cells in hamster feed arteries: role in vasomotor control. Circulation research. 2000 Sep 15; 87(6):474–479. [PubMed: 10988239]
33. Siegl D, Koeppen M, Wolfle SE, Pohl U, de Wit C. Myoendothelial coupling is not prominent in arterioles within the mouse cremaster microcirculation in vivo. Circulation research. 2005 Oct 14; 97(8):781–788. [PubMed: 16166558]
34. Knot HJ, Nelson MT. Regulation of membrane potential and diameter by voltage-dependent K+ channels in rabbit myogenic cerebral arteries. The American journal of physiology. 1995 Jul; 269(1 Pt 2):H348–355. [PubMed: 7631867]

35. Herrera GM, Heppner TJ, Nelson MT. Voltage dependence of the coupling of Ca(2+) sparks to BK(Ca) channels in urinary bladder smooth muscle. Am J Physiol Cell Physiol. 2001 Mar; 280(3):C481–490. [PubMed: 11171567]

36. Burdyga T, Wray S. Action potential refractory period in ureter smooth muscle is set by Ca sparks and BK channels. Nature. 2005 Jul 28; 436(7050):559–562. [PubMed: 16049489]

37. Lifshitz LM, Carmichael JD, Lai FA, et al. Spatial organization of RYRs and BK channels underlying the activation of STOCs by Ca(2+) sparks in airway myocytes. The Journal of general physiology. 2011 Aug; 138(2):195–209. [PubMed: 21746845]

38. Lu T, Ye D, He T, Wang XL, Wang HL, Lee HC. Impaired Ca2+-dependent activation of large-conductance Ca2+-activated K+ channels in the coronary artery smooth muscle cells of Zucker Diabetic Fatty rats. Biophys J. 2008 Dec; 95(11):5165–5177. [PubMed: 18790848]

39. Amberg GC, Bonev AD, Rossow CF, Nelson MT, Santana LF. Modulation of the molecular composition of large conductance, Ca(2+) activated K(+) channels in vascular smooth muscle during hypertension. J Clin Invest. 2003 Sep; 112(5):717–724. [PubMed: 12952920]

40. Mokelke EA, Dietz NJ, Eckman DM, Nelson MT, Sturek M. Diabetic dyslipidemia and exercise affect coronary tone and differential regulation of conduit and microvessel K+ current. Am J Physiol Heart Circ Physiol. 2005 Mar; 288(3):H1233–1241. [PubMed: 15528227]

41. Kalyanaraman B, Darley-Usmar V, Davies KJ, et al. Measuring reactive oxygen and nitrogen species with fluorescent probes: challenges and limitations. Free radical biology & medicine. 2012 Jan 1; 52(1):1–6. [PubMed: 22027063]

42. Rota C, Chignell CF, Mason RP. Evidence for free radical formation during the oxidation of 2′-7′-dichlorofluorescin to the fluorescent dye 2′-7′-dichlorofluorescein by horseradish peroxidase: possible implications for oxidative stress measurements. Free radical biology & medicine. 1999 Oct; 27(7-8):873–881. [PubMed: 10515592]

43. Ethier MF, Madison JM. LY294002, but not wortmannin, increases intracellular calcium and inhibits calcium transients in bovine and human airway smooth muscle cells. Cell calcium. 2002 Jul; 32(1):31–38. [PubMed: 12127060]

Europe PMC Funders Author Manuscripts

Europe PMC Funders Author Manuscripts

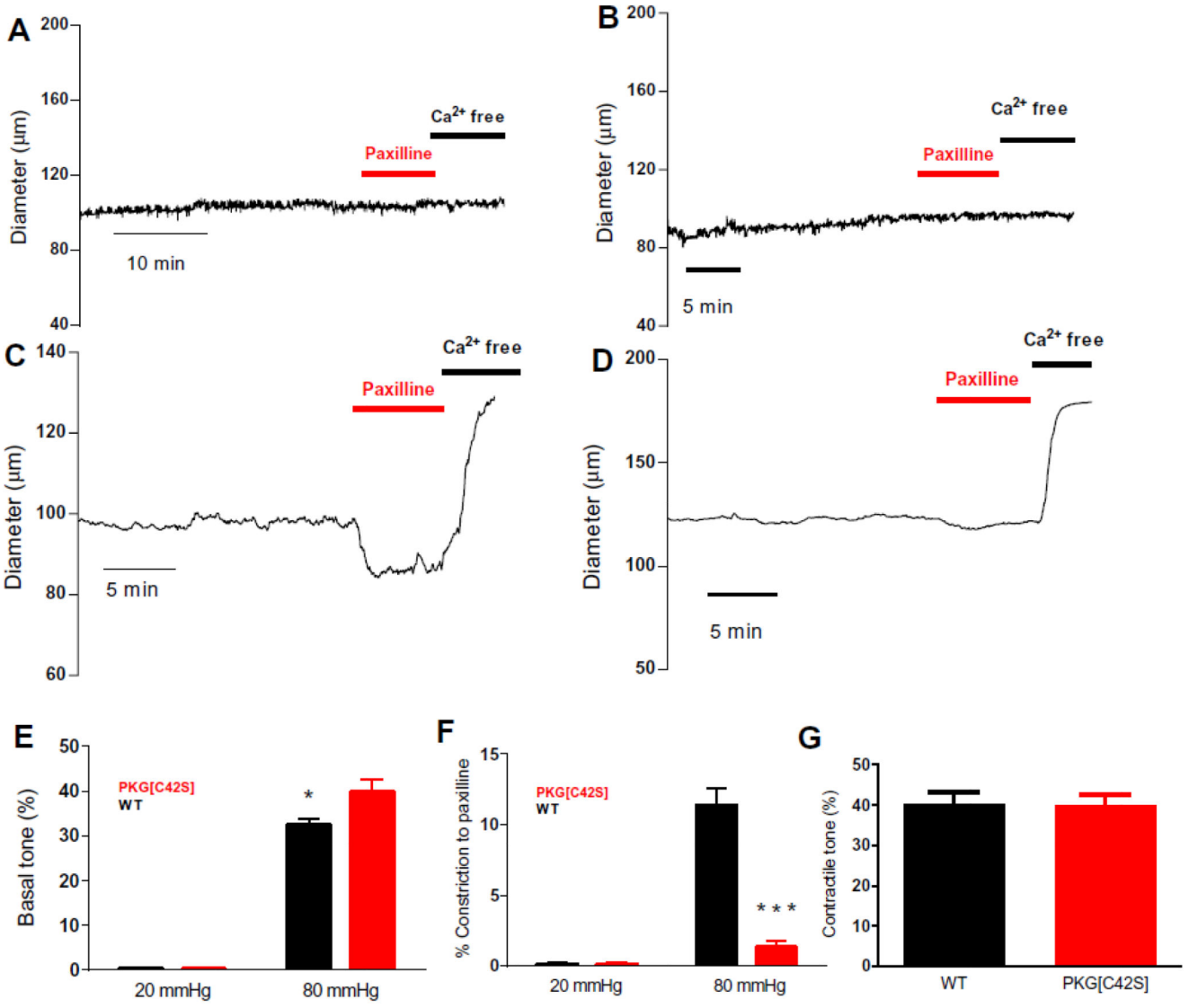

Figure 1. Intravascular pressure activates oxidizable PKG, which engages BK channels to oppose tone development.

A and B: Representative diameter traces from WT (A) and PKG[C42S]^{KI} (B) mesenteric arteries pressurized to 20 mmHg. C and D: Representative diameter trace from WT (C) and PKG[C42S]^{KI} (D) mesenteric arteries pressurized to 80 mmHg. E: Pressure-induced constriction in PKG[C42S]^{KI} and WT arteries measured at 20 and 80 mmHg. Percent constriction of PKG[C42S]^{KI} arteries (39.8% ± 2.5%, n = 20 arteries from 12 mice) was significantly greater than WT arteries (32.4% ± 1.2%, n = 27 arteries from 19 mice) at 80 mmHg intraluminal pressure. P=0.014, Mann-Whitney U test. Absolute active diameters: WT: 108.4 ± 3.3µm; PKG[C42S]^{KI}: 99.8 ± 6.7µm. Absolute passive diameters: WT: 161.1 ± 4.7µm; PKG[C42S]^{KI}: 161.2 ± 5.9µm. F: Response to paxilline in PKG[C42S]^{KI} and WT arteries measured at 20 and 80 mmHg. Percent constriction (relative to passive diameter) in response to paxilline in WT arteries (11.4% ± 1.8%, n = 6 arteries from 6 mice) was significantly greater than in PKG[C42S]^{KI} arteries (1.3% ± 0.6%, n = 5 arteries from 5

mice) at 80 mmHg intraluminal pressure. $P = 0.002$, unpaired t-test. G: Degree of pressure-induced constriction in untreated arteries from PKG[C42S]^{KI} mice (39.8% ± 2.5%, n = 20 arteries from 12 mice) was not significantly different from that in paxilline (Pax)-treated arteries from WT mice (40.1% ± 3%, n = 6 arteries from 6 mice).

Europe PMC Funders Author Manuscripts

Europe PMC Funders Author Manuscripts

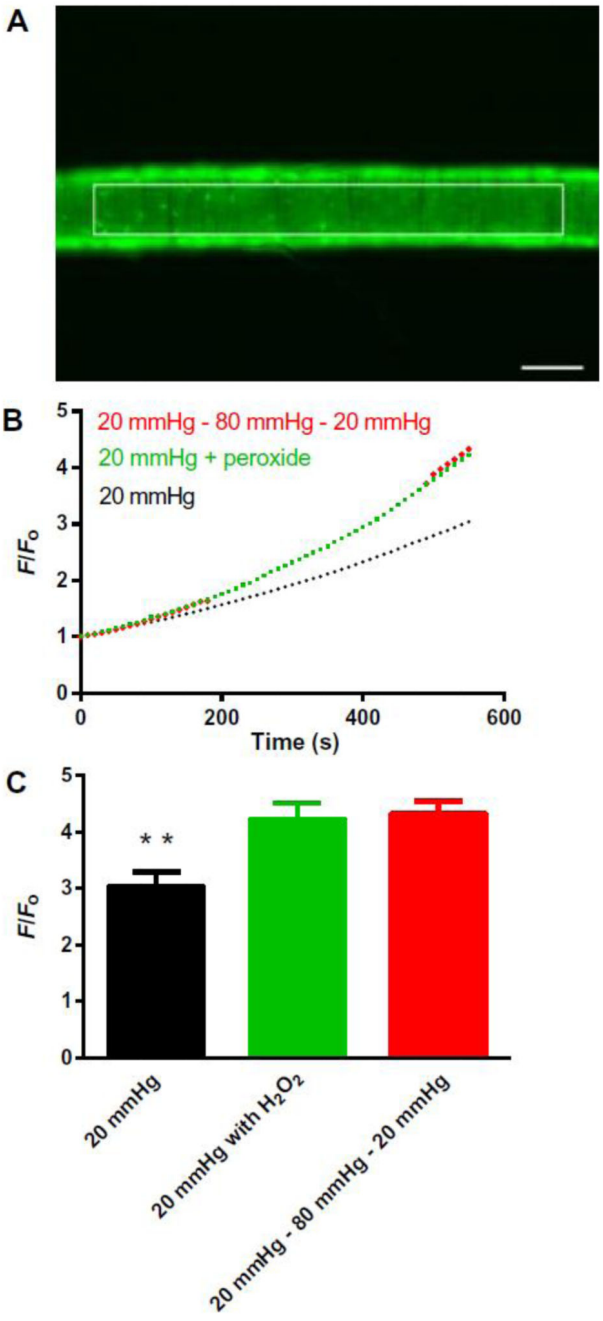

Figure 2. Intraluminal pressure increases oxidant amounts in mesenteric arteries.

A: Representative example of a third-order mesenteric artery loaded with CM-DCF and pressurized at 20 mmHg showing the region of interest (ROI). White scale bar: 100 μm. B: Averaged traces (SEM bars omitted) showing the rate of the increase in fluorescence in CM-DCF–loaded WT arteries continuously pressurized to 20 mmHg (black line; n = 4 arteries from 4 mice); continuously pressurized to 20 mmHg with exogenous application of the antioxidant H_2O_2 (30 μM), added at 240 seconds (red line; n = 4 arteries from 4 mice); and pressurized initially to 20 mmHg and then stepped to 80 mmHg at 210 seconds, and back to

Europe PMC Funders Author Manuscripts

20 mmHg at 480 seconds (green line: n=4 arteries from 4 mice). Dotted green line reflects artifactual changes in fluorescence caused by movement of the artery out of the focal plane. Representative traces for each protocol are shown in Supplementary Figure 3. C: End point (at 10 minutes) comparisons of increases in F/F_0 for control arteries continuously pressurized to 20 mmHg (F/F_o = 3.0 ± 0.3; n = 4 arteries from 4 mice), continuously pressurized to 20 mmHg with exogenous addition of H_2O_2 (F/F_o = 4.2 ± 0.3; n = 4 arteries from 4 mice), and subjected to a pressure-step protocol from 20 to 80 to 20 mmHg (F/F_o = 4.3 ± 0.2; n = 4 arteries from 4 mice), presented as means ± SEM. **P* = 0.01, compared with control at 20 mmHg.

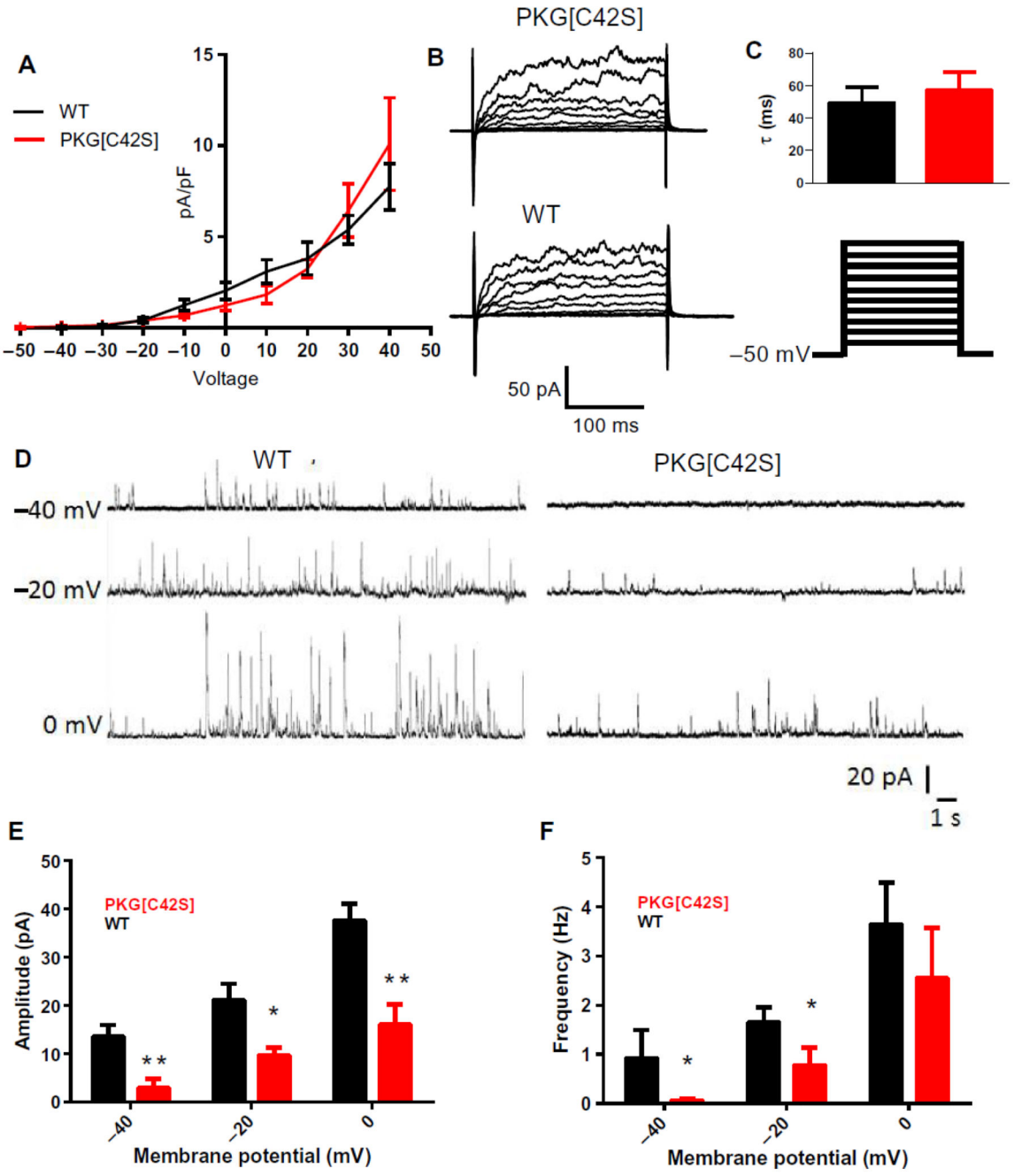

Figure 3. Oxidant activation of PKG controls BK channel function indirectly through effects on STOCs.

A: Current density–voltage plots comparing BK channel currents (paxilline-sensitive difference currents) between VSMCs from WT (black line; n = 6 cells from 3 mice) and PKG[C42S]^{KI} (red line; n = 7 cells from 3 mice) mesenteric arteries. B. Representative voltage-step current recordings from WT and PKG[C42S]^{KI} arteries. C: BK current activation constant (τ) were not significantly different in VSMCs from WT mice (49.4 ± 9.6 ms, n = 4 cells from 2 mice) and PKG[C42S]^{KI} mice (57.1 ± 11.3 ms, n = 4 cells from 3 mice), calculated between -50 and 50 mV. D: Representative perforated patch-clamp

recordings from isolated VSMCs from WT (left) and PKG[C42S]^{KI} (right) mesenteric arteries. E and F: STOC amplitude (E) and frequency (F) in myocytes from WT (-40mV: n=6 cells from 3 mice, -20mV: n=6 cells from 3 mice, 0mV: n=6 cells from 3 mice), and PKG[C42S]^{KI} (-40mV: n = 6 cells from 3 mice, -20mV: n = 10 cells from 7, mice, 0Mv: n = 5 cells from 3 mice) mesenteric arteries, presented as means ± SEM. *$P < 0.05$: WT compared to PKG[C42S]^{KI} for STOC amplitudes at all membrane potentials using unpaired t-test and for STOC frequency at -40mV and -20mV using Mann-Whitney U test.

Europe PMC Funders Author Manuscripts

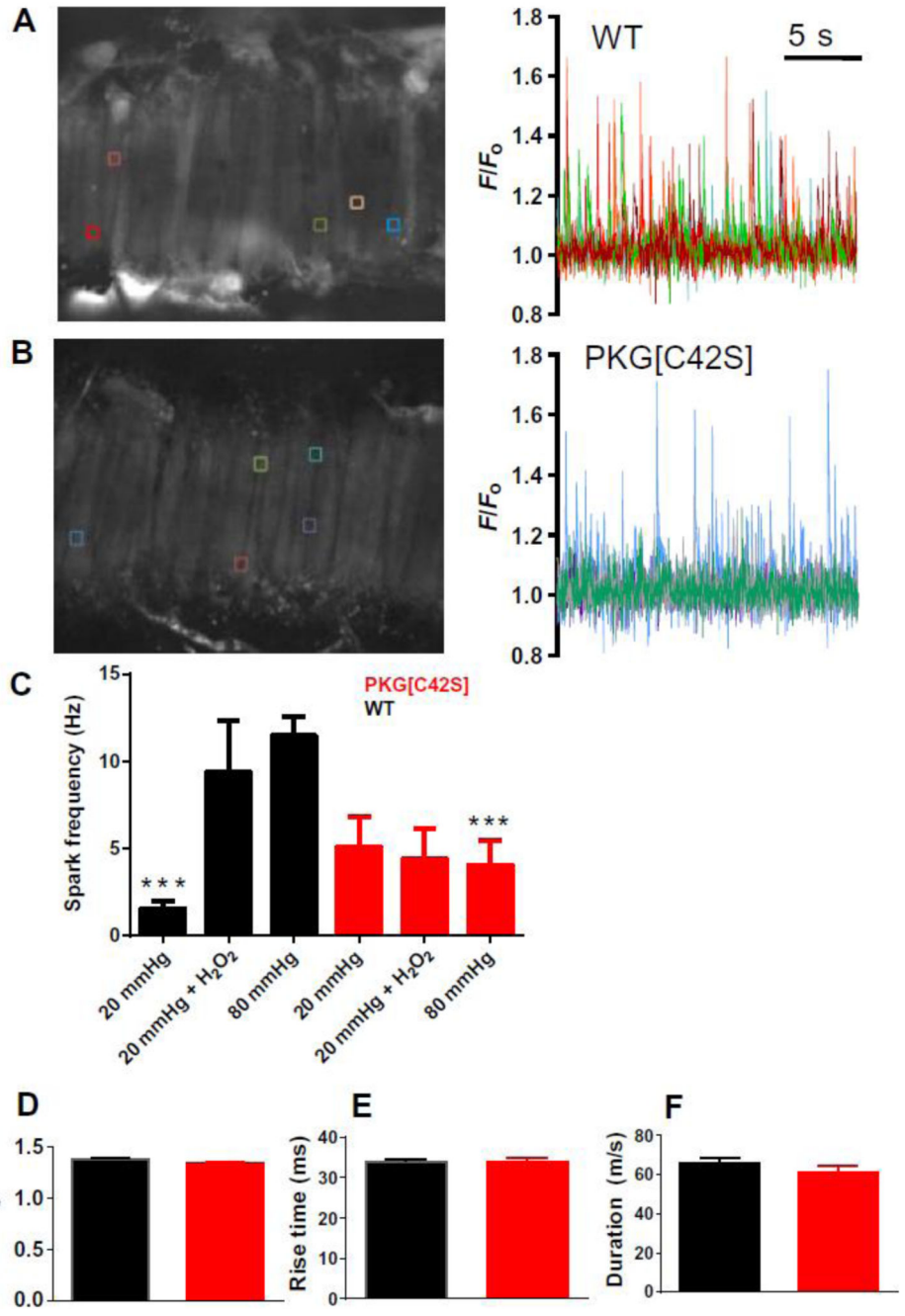

Figure 4. Ca^{2+} spark frequency is reduced in $PKG[C42S]^{KI}$ mesenteric arteries.

A and B: Ca^{2+} spark activity in WT (A) and $PKG[C42S]^{KI}$ (B) arteries pressurized to 80 mmHg. Left: Representative images of Ca^{2+} sparks in arteries, visualized using a confocal spinning-disc microscope. Right: Colored lines indicating changes in fractional fluorescence (F/F_0) at individual ROIs corresponding to the boxes of the same color in fields shown in the image at left. C: Ca^{2+} spark frequencies in WT and $PKG[C42S]^{KI}$ arteries measured within an entire field of view (comprising around 15 adjacent cells) at 20 mmHg (WT, n = 7 arteries from 7 mice; $PKG[C42S]^{KI}$, n =6 arteries from 5 mice), 20 mmHg in the presence of

30 μM H_2O_2 (WT, n = 7 arteries from 2 mice; PKG[C42S]^{KI}, n = 6 arteries from 2 mice), and 80 mmHg (WT, n = 8 arteries from 7 mice; PKG[C42S]^{KI}, n = 14 arteries from 11 mice). Data are presented as means ± SEM. $P = 0.002$, for WT compared to PKG[C42S]^{KI} at 80 mmHg; $P < 0.01$, for WT at 80 mmHg compared to WT at 20 mmHg; $P = 0.04$ for WT at 20 mmHg+H_2O_2 compared to WT at 20 mmHg, all t-test. Ca^{2+} spark frequency in PKG[C42S]^{KI} arteries was unaffected by pressure or H_2O_2.

Europe PMC Funders Author Manuscripts